Identification of Target Integrin Thyroid Hormone Receptors from Sea Urchins

Submission Date:
Tuesday, August 12, 2025

Prepared By:
Dilma Karunathilake, 0969209
*For BINF*6999: Bioinformatics Master's Project*

Advisors:
Dr. Andreas Heyland, Professor, Department of Integrative Biology, University of Guelph, Guelph, ON N1G 2W1, Canada. *(Biological Advisor)*
Dr. Rui Huang, Assistant Professor, Department of Chemistry, University of Guelph, Guelph, ON N1G 2W1, Canada. *(Informatics Advisor)*

Table of Contents

Abstract

Integrin αVβ3 is a well-characterized non-canonical receptor for thyroid hormones (TH) in vertebrates, yet echinoderms lack a direct β3 ortholog. I hypothesized that conserved or structurally analogous sea urchin integrins could form comparable TH-binding pockets with ligand selectivity patterns resembling αVβ3. Six *Strongylocentrotus purpuratus* heterodimers (αVβG, αVβ1-A, αVβC, αPβG, αPβ1-A, αPβC) were modeled using AlphaFold-Multimer, with human αVβ3 serving as a reference. Model confidence was evaluated via pLDDT, pTM, ipTM, and RMSD to the αVβ3 crystal structure (PDB 1L5G). High-confidence extracellular domain predictions enabled in-silico docking in HADDOCK against cyclic RGD and seven TH metabolites (rT3, T4, T3, TRIAC, TETRAC, sT3, sT4), followed by binding free energy (ΔG) and dissociation constant (K_D) estimation in PRODIGY. Among sea urchin integrins, αPβ1-A most closely matched αVβ3 binding behavior, showing sub-micromolar affinity for all ligands and low-nanomolar affinity for sT3 and sT4. αPβG and αVβ1-A also displayed strong binding profiles, whereas βC-containing dimers showed greater structural divergence and weaker, more variable affinities. These findings identify αPβ1-A as the strongest candidate for a functional analog of αVβ3 in *S. purpuratus*, consistent with prior evidence that THs bind sea urchin membranes and regulate gene expression. This study supports the hypothesis that integrin-mediated, non-canonical TH signaling is an evolutionarily conserved feature and provides a computational framework for predicting functional analogs in species lacking direct orthologs.

Introduction

Integrins are a large family of heterodimeric transmembrane receptors that mediate cell adhesion, migration, and signaling by linking the extracellular matrix (ECM) to the cytoskeleton (Takada et al., 2007). Each integrin consists of a non-covalently associated α- and β-subunit, with the extracellular regions forming a ligand-binding headpiece supported by leg-like stalk domains that span the plasma membrane and connect to short cytoplasmic tails (Takada et al., 2007). The extracellular α-subunit typically contains a β-propeller domain, while the β-subunit contains a β-I (also known as βA) domain, which together form the integrin head responsible for ligand recognition and coordination of divalent cations at the metal-ion–dependent adhesion site (MIDAS) (Rothman, 2022). These cations (often Mn^{2+}, Mg^{2+}, or Ca^{2+}) are critical for ligand binding and structural stability (Tiwari et al., 2011).

A well-studied subset of integrins are those that recognize the Arg-Gly-Asp (RGD) tripeptide motif, which is found in numerous ECM proteins such as fibronectin, vitronectin, and fibrinogen (Ludwig et al., 2021). RGD-binding integrins include αVβ3, αVβ5, αIIbβ3, and several α5-containing heterodimers (Ludwig et al., 2021). In human αVβ3, the RGD motif binds by inserting the arginine into a deep pocket in the α-subunit β-propeller domain, while the aspartate coordinates with the β-subunit MIDAS cation (Xiong et al., 2002). The crystal structure of the extracellular segment of human αVβ3 in complex with a cyclic RGD ligand (PDB ID: 1L5G) has provided a detailed view of this interaction (Xiong et al., 2002). In 1L5G, the αV β-propeller domain and β3 β-I domain form a complementary interface that precisely positions the RGD ligand, and the structure also reveals the coordination geometry of the Mn^{2+} and Ca^{2+} ions that stabilize the ligand-receptor complex. This high-resolution structural information has made αVβ3 a model system for studying RGD-binding integrins and for guiding molecular docking experiments.

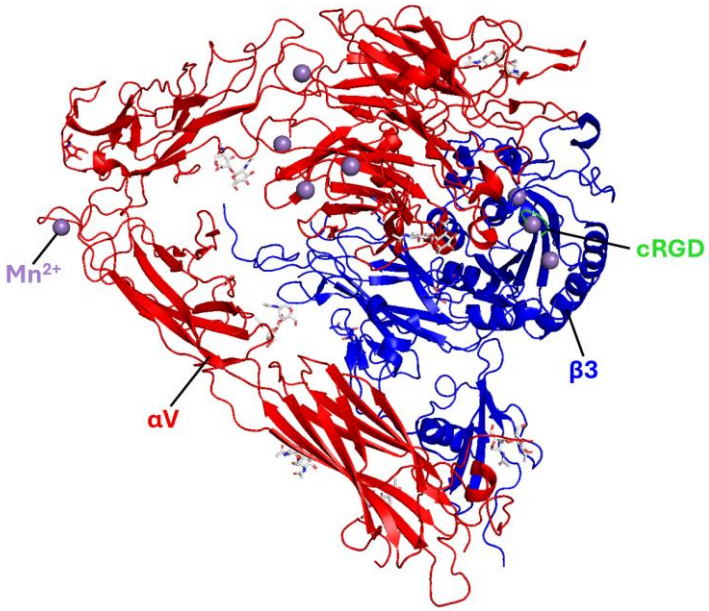

Figure 1. *Crystal structure of the extracellular segment of human integrin αVβ3 in complex with a cyclic RGD (cRGD) ligand (PDB ID: 1L5G).* The αV subunit (red) contains the β-propeller domain that engages the arginine residue of the RGD motif, while the β3 subunit (blue) contributes its β-I domain, coordinating the aspartate via the MIDAS site. The cRGD ligand is shown in green, and bound Mn^{2+} ions (purple) highlight divalent cation coordination essential for ligand binding and structural stability.

Beyond classical ECM ligands, αVβ3 has also been shown to bind small molecules, including thyroid hormones (THs), through a site distinct from the canonical RGD-binding pocket (Tobi et al., 2022). Triiodothyronine (T3) and thyroxine (T4), along with several thyroid hormone metabolites, can interact with αVβ3, triggering non-genomic signaling pathways involved in cell proliferation, angiogenesis, and cancer progression. Docking and mutagenesis studies indicate that the TH-binding site is located near, but not identical to, the RGD site, with possible allosteric crosstalk between the two (Tobi et al., 2022). This dual-ligand recognition capability of αVβ3 suggests a broader functionality for these integrins than previously recognized.

In echinoderms such as the purple sea urchin (*Strongylocentrotus purpuratus*), genomic surveys have identified a number of α- and β-subunits, but direct structural or biochemical characterization of their ligand-binding properties remains limited. Sea urchins present an interesting case because thyroid hormones have been shown to accelerate skeletogenesis during larval development (Taylor

et al., 2023). Experimental work has demonstrated TH binding activity in sea urchin membrane preparations, along with transcriptional regulation of downstream targets in response to TH exposure (Taylor et al., 2023; Tieman, 2025). However, the identity of the membrane receptor(s) mediating this effect remains unknown. Given the structural and functional parallels between human αVβ3 and certain echinoderm integrins, it is plausible that one or more sea urchin integrins act as functional analogs capable of binding THs in a similar manner.

The β-propeller domain of α-subunits and β-I domain of β-subunits are key determinants of ligand specificity (Rothman, 2022). Therefore, identifying sea urchin α–β heterodimers with conserved or structurally analogous domain arrangements to human αVβ3 could highlight candidate receptors for TH binding. In particular, β-subunits with conserved MIDAS motifs and α-subunits with RGD-compatible β-propeller topologies may be predisposed to accommodate thyroid hormone metabolites.

Despite these clues, there is currently a gap in knowledge as there have been no studies that have systematically modeled full-length sea urchin integrins and compared their predicted TH-binding capabilities to human αVβ3. Moreover, while human αVβ3 has been characterized crystallographically, sea urchin structures have only been inferred from sequence data, without experimental validation. There has also been no in-silico screenings across multiple sea urchin integrins to assess which candidates may best replicate αVβ3's dual-binding capabilities with RGD and thyroid hormones.

The objective of this study was to fill this gap by generating high-confidence structural models of six sea urchin integrin heterodimers (αVβG, αVβ1-A, αVβC, αPβG, αPβ1-A, and αPβC) using AlphaFold, with the human αVβ3 crystal structure (PDB ID: 1L5G) as a structural reference. These models were then put through docking analyses using HADDOCK to assess binding with seven key ligands: the cyclic RGD peptide (cRGD), T3, T4, reverse T3 (rT3), triiodothyroacetic acid (TRIAC),

tetraiodothyroacetic acid (TETRAC), and sulfated derivatives sT3 and sT4. Binding affinities were estimated using PRODIGY, and results were compared to identify which sea urchin integrins most closely replicate αVβ3's binding profile.

It was hypothesized that conserved or structurally analogous sea urchin integrin subunits form thyroid hormone binding pockets with varying selectivity for different thyroid hormone metabolites. By integrating structural modeling, molecular docking, and binding affinity prediction, this study aims to pinpoint likely functional analogs of αVβ3 in *S. purpuratus* and provide a computational framework for guiding future experimental validation.

Methods

Dataset Acquisition and Selection

Protein sequences for sea urchin (*Strongylocentrotus purpuratus*) integrin subunits of interest, αV (LOC583516), αP (LOC373206), βG (LOC373367), β1A (LOC767502), and βC (LOC373364), were obtained from Echinobase, which links to NCBI FASTA entries. These monomers were selected based on prior identification by the Heyland Lab as potentially relevant to non-canonical thyroid hormone (TH) signaling. For a reference model, the crystal structure of the human αVβ3 integrin (PDB ID: 1L5G) containing eight Mn^{2+} ions and the cyclic RGD (cRGD) ligand Cilengitide was retrieved from the Protein Data Bank (PDB). Full-length human αV (P06756) and β3 (P05106) sequences were obtained from UniProt to ensure complete modeling of the integrin heterodimer, as PDB 1L5G contains only the extracellular domain. Multiple sequence alignment (MSA) was performed in ClustalW and visualized in ESPript to confirm inclusion of residues from 1L5G in the UniProt sequences.

Structure Prediction

The full-length αVβ3 integrin containing eight Mn^{2+} ions was modeled using AlphaFold-Multimer. Among the five generated models, the one with the highest predicted Local Distance Difference Test (pLDDT), predicted Template Modeling score (pTM), and interface predicted TM-score (ipTM) was selected. Structural alignment with PDB 1L5G was performed in PyMOL (using the super command), yielding a root-mean-square deviation (RMSD) of 1.052 Å, confirming model accuracy. The same AlphaFold-Multimer workflow was applied to generate models of six sea urchin integrin heterodimers: αVβG, αVβ1A, αVβC, αPβG, αPβ1A, and αPβC. For each dimer, the best-scoring model was selected. A custom Python script converted AlphaFold .cif files to .pdb and extracted model scores.

Structure Preparation for Docking

AlphaFold models were preprocessed for HADDOCK 2.5 compatibility. Because HADDOCK does not support duplicate residue numbering, a Python script was used to renumber residues sequentially across chains. Another script inserted ion charges into the third PDB column for Mn^{2+} entries. Key residues in αVβ3 known to interact with cRGD (Asp150, Asp218 in αV; Ser121, Tyr122, Ser123, Arg214, Asn215, Glu220 in β3) were identified from Xiong et al. (2002). These residues were mapped to the sea urchin models via PyMOL alignment and visual inspection for use as active residues in HADDOCK docking (seen in Table 1). Ligand files were obtained from PubChem and Zinc15 and converted to .pdb files using OpenBabel.

Docking Simulations

Docking was performed in HADDOCK 2.5 for each integrin dimer with eight ligands: seven TH metabolites (rT3, T3, T4, sT3, sT4, TRIAC, TETRAC) and cRGD. For cRGD, active residues 1 (Arg) and 3 (Asp) were specified as ligand residues, and active residues for TH metabolites were taken from their specific PDB atom listings (seen in Table 1). Integrin active residues were those identified in the mapping step done previously. The best model from the top HADDOCK cluster was selected for each docking run based on HADDOCK score, cluster size, RMSD from the lowest-energy structure, Van der Waals energy, electrostatic energy, desolvation energy, restraints violation energy, buried surface area, and Z-score.

Binding Affinity Estimation

Top docked models were processed in PRODIGY to predict binding free energies (ΔG, $kcal \cdot mol^{-1}$). For T3-containing PDB files, a preprocessing script converted ligand records from ATOM to HETATM and changed residue name from “T3” to “LIG” to ensure PRODIGY compatibility. Dissociation

constants (Kd) were calculated from ΔG values using the equation $\Delta G = RT \ln (K_d)$ and the constants R (gas constant) = 0.001987 kcal·mol^{-1}·K^{-1} and T (absolute temperature) = 298.15 K (25 °C).

Visualization

For AlphaFold models, a script containing a pLDDT-based coloring scheme was applied in PyMOL. Final docked complexes were also visualized in PyMOL to illustrate ligand placement relative to the RGD-binding site.

All supplementary materials, including data files and custom Python scripts used in the workflow, are available on my GitHub repository at: *[https://github.com/dkarunat123/MBinf_Identification-of-Target-Integrin-Thyroid-Hormone-Receptors-from-Sea-Urchins]*.

Key Interacting Residues	
Integrin Residues	**Ligand Residues**
PDB 1l5g: αVβ3	**cRGD**
150, 218, 121, 122, 123, 214, 215, 220	1, 3
αVβ3	**rT3**
180, 248, 1195, 1196, 1197, 1288, 1289, 1294	1
αVβG	**TRIAC**
229, 257, 1043, 1044, 1045, 1131, 1132, 1137	1
αVβC	**TETRAC**
204, 257, 1053, 1054, 1055, 1142, 1143, 1148	1
αVβ1-A	**T3**
204, 257, 1048, 1049, 1050, 1136, 1137, 1142	500
αPβG	**T4**
178, 234, 1198, 1199, 1200, 1286, 1287, 1292	1008
αPβC	**sT3**
264, 289, 1208, 1209, 1210, 1334, 1335, 1340	1
αPβ1-A	**sT4**
178, 234, 1203, 1204, 1205, 1291, 1292, 1297	1

Table 1. *Key interacting residues for each integrin–ligand pair used in HADDOCK docking.* Integrin residues for human αVβ3 (PDB 1L5G) were obtained from Xiong et al. (2002) and mapped to the corresponding residues in modeled human and sea urchin integrins via PyMOL alignment. Ligand residues correspond to the .pdb file-specific active sites specified for cRGD and thyroid hormone metabolites (rT3, T3, T4, sT3, sT4, TRIAC, TETRAC).

Results

AlphaFold Modeling Results of Human and Sea Urchin Integrins

AlphaFold-Multimer was used to generate full-length structural models of human αVβ3 and six sea urchin integrin heterodimers. Model quality was assessed using three confidence metrics provided by AlphaFold (predicted Local Distance Difference Test (pLDDT), predicted Template Modeling score (pTM), and interface pTM score (ipTM)) as well as structural alignment to the crystal structure of human αVβ3 (PDB 1L5G) using PyMOL's *super* command to calculate RMSD.

The pLDDT score measures per-residue confidence in the model (0–100 scale), with scores above 90 indicating very high accuracy, 70–90 indicating confident prediction, 50–70 suggesting low confidence, and below 50 reflecting likely disorder (Jumper et al., 2021). All models had mean pLDDT values between 74.01 and 81.29, placing them in the 'confident prediction' range, with the human αVβ3 model achieving the highest value (81.29). pTM assesses the accuracy of the global fold (0–1 scale), with values above 0.7 typically indicating a correct overall topology (Jumper et al., 2021). ipTM, also on a 0–1 scale, evaluates the accuracy of the inter-chain interface, with values above 0.7 considered reliable for protein–protein interactions. The human αVβ3 model, once again, scored highest for both pTM (0.82) and ipTM (0.81), supporting its use as a reference structure. Among the sea urchin integrins, αVβ1-A (pTM 0.69, ipTM 0.72) showed the strongest predicted structural integrity at the subunit interface, while αPβC had the lowest scores (pTM 0.63, ipTM 0.62).

Structural alignment of the full-length models to the αVβ3 extracellular crystal structure (PDB 1L5G) provided RMSD values that reflected overall similarity in fold and domain arrangement. The human αVβ3 model aligned closely to the crystal structure (RMSD 1.052 Å), confirming its validity as a substitute for the extracellular-only αVβ3 crystal structure. Among sea urchin integrins, αVβG (3.053 Å) and αPβG (3.629 Å) aligned most closely, followed by αVβ1-A (3.717 Å) and αPβ1-A (4.331 Å). The βC-containing heterodimers αVβC (4.086 Å) and αPβC (8.467 Å) deviated most from the αVβ3

reference, with αPβC showing substantial structural divergence. These deviations were also visually apparent, as βC-containing dimers displayed altered domain orientations and partial loss of the canonical headpiece–leg arrangement compared to the other integrins.

All models were colored by pLDDT score, with dark blue indicating very high confidence, cyan high confidence, yellow low confidence, and orange very low confidence. The main extracellular ligand-binding regions of all integrins were predominantly dark blue or cyan, indicating high prediction accuracy in the β-propeller and β-I domains of the α-subunit and the β-I domain of the β-subunit. Lower-confidence regions (yellow/orange) were generally located in flexible or peripheral domains, such as distal leg regions, that are not directly involved in ligand recognition. However, Mn^{2+}-binding sites in most integrin models displayed slightly reduced pLDDT scores relative to surrounding residues, indicating uncertainty in precise ion positioning. This was particularly notable in the αPβ1-A model, where one Mn^{2+} ion was positioned differently compared to the canonical locations observed in human αVβ3.

Overall, the AlphaFold models provided high-confidence predictions for the main extracellular architecture of both human and sea urchin integrins, enabling their use in the subsequent docking workflow. The structural similarity of αVβG, αPβG, αVβ1-A, and αPβ1-A to human αVβ3, along with their preservation of the ligand-binding headpiece, suggested that these integrins might exhibit docking behaviors more comparable to αVβ3 than the structurally divergent βC-containing dimers.

Human αVβ3

A

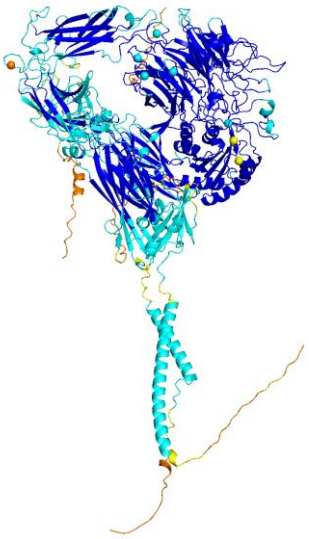

ipTM: 0.81
pTM: 0.82
plDDT: 81.29
RMSD: 1.052

Figure 2: *AlphaFold-Multimer models of human and sea urchin integrin heterodimers.* **(A)** AlphaFold model of the human αVβ3 integrin with its ipTM, pTM, and pLDDT scores and an RMSD score for its alignment with PDB 1L5G (the crystal structure of the αVβ3 extracellular domain). **(B–D)** Sea urchin αVβG, αVβ1-A, and αVβC AlphaFold models and their respective confidence scores and RMSD values when aligned to PDB 1L5G. **(E–G)** ipTM, pTM, and pLDDT scores and an RMSD score for alignment with PDB 1L5G for sea urchin αPβG, αPβ1-A, and αPβC models.

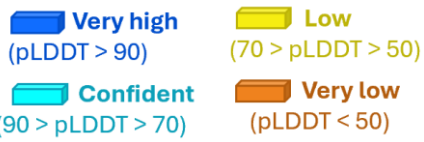

Sea Urchin αVβG | **Sea Urchin αVβ1-A** | **Sea Urchin αVβC**

B

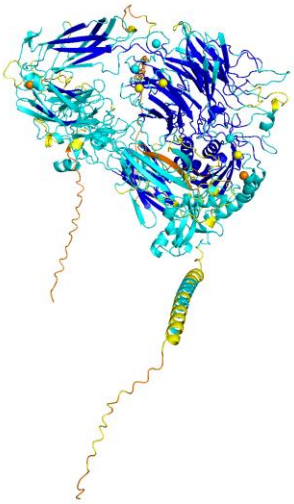

ipTM: 0.67
pTM: 0.64
plDDT: 75.55
RMSD: 3.053

C

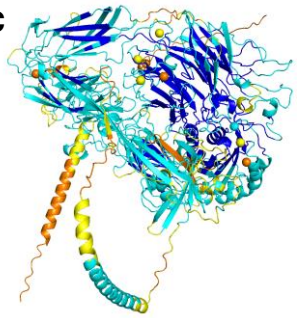

ipTM: 0.72
pTM: 0.69
plDDT: 74.44
RMSD: 3.717

D

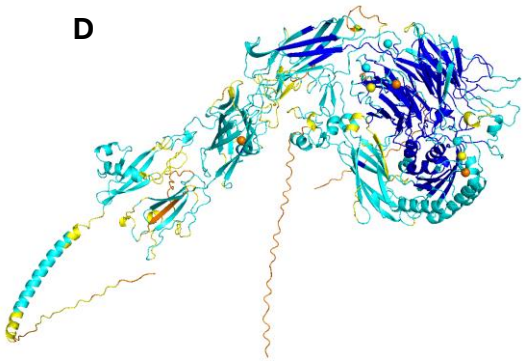

ipTM: 0.67
pTM: 0.63
plDDT: 74.01
RMSD: 4.086

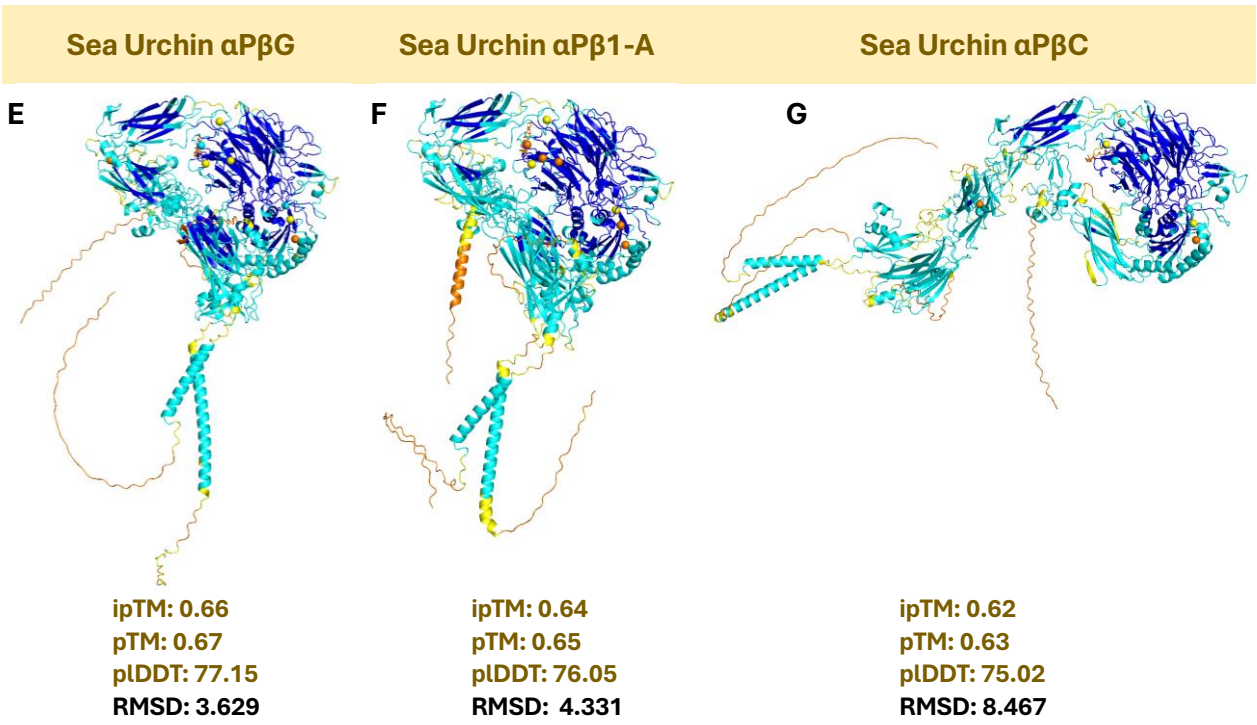

HADDOCK & PRODIGY Docking Results for cRGD and Thyroid Hormone Metabolites

Docking results were evaluated using predicted binding free energy (ΔG) scores from PRODIGY and dissociation constant (K_D) values calculated from the ΔG values. ΔG, expressed in kcal/mol, reflects the thermodynamic favourability of the ligand–receptor interaction, with more negative values indicating stronger predicted binding . K_D, expressed in micromolar units (μM), represents the equilibrium concentration at which half of the receptor sites are bound by the ligand, where lower K_D values correspond to higher binding affinity (Borea et al., 1998). In general, ΔG values below −9.0 kcal/mol and K_D values in the low micromolar to nanomolar range are indicative of strong binding, whereas higher ΔG and K_D values suggest weaker interactions (Borea et al., 1998).

Integrin	cRGD	TRIAC	TETRAC	rT3
αVβ3	**ΔG = -9.68** K_{cal}/mol **K_D = 0.080** μM	**ΔG = -10.68** K_{cal}/mol **K_D = 0.015** μM	**ΔG = -10.40** K_{cal}/mol **K_D = 0.024** μM	**ΔG = -9.27** K_{cal}/mol **K_D = 0.160** μM
αVβG	**ΔG = -8.19** K_{cal}/mol **K_D = 0.991** μM	**ΔG = -10.05** K_{cal}/mol **K_D = 0.043** μM	**ΔG = -9.89** K_{cal}/mol **K_D = 0.056** μM	**ΔG = -8.81** K_{cal}/mol **K_D = 0.348** μM
αVβ1-A	**ΔG = -8.89** K_{cal}/mol **K_D = 0.304** μM	**ΔG = -10.17** K_{cal}/mol **K_D = 0.035** μM	**ΔG = -10.18** K_{cal}/mol **K_D = 0.034** μM	**ΔG = -9.06** K_{cal}/mol **K_D = 0.228** μM
αVβC	**ΔG = -9.02** K_{cal}/mol **K_D = 0.244** μM	**ΔG = -10.05** K_{cal}/mol **K_D = 0.043** μM	**ΔG = -9.80** K_{cal}/mol **K_D = 0.065** μM	**ΔG = -9.12** K_{cal}/mol **K_D = 0.206** μM
αPβG	**ΔG = -9.64** K_{cal}/mol **K_D = 0.086** μM	**ΔG = -10.13** K_{cal}/mol **K_D = 0.037** μM	**ΔG = -10.31** K_{cal}/mol **K_D = 0.028** μM	**ΔG = -9.37** K_{cal}/mol **K_D = 0.135** μM
αPβ1-A	**ΔG = -10.13** K_{cal}/mol **K_D = 0.037** μM	**ΔG = -10.55** K_{cal}/mol **K_D = 0.018** μM	**ΔG = -10.57** K_{cal}/mol **K_D = 0.018** μM	**ΔG = -9.81** K_{cal}/mol **K_D = 0.064** μM
αPβC	**ΔG = -9.45** K_{cal}/mol **K_D = 0.118** μM	**ΔG = -10.52** K_{cal}/mol **K_D = 0.019** μM	**ΔG = -8.36** K_{cal}/mol **K_D = 0.744** μM	**ΔG = -9.27** K_{cal}/mol **K_D = 0.160** μM
Integrin	**T3**	**T4**	**sT3**	**sT4**
αVβ3	**ΔG = -9.87** K_{cal}/mol **K_D = 0.058** μM	**ΔG = -9.83** K_{cal}/mol **K_D = 0.062** μM	**ΔG = -11.46** K_{cal}/mol **K_D = 0.004** μM	**ΔG = -11.07** K_{cal}/mol **K_D = 0.008** μM
αVβG	**ΔG = -8.90** K_{cal}/mol **K_D = 0.299** μM	**ΔG = -8.97** K_{cal}/mol **K_D = 0.266** μM	**ΔG = -10.45** K_{cal}/mol **K_D = 0.022** μM	**ΔG = -10.30** K_{cal}/mol **K_D = 0.028** μM
αVβ1-A	**ΔG = -9.35** K_{cal}/mol **K_D = 0.140** μM	**ΔG = -9.69** K_{cal}/mol **K_D = 0.079** μM	**ΔG = -10.82** K_{cal}/mol **K_D = 0.012** μM	**ΔG = -10.36** K_{cal}/mol **K_D = 0.025** μM
αVβC	**ΔG = -9.48** K_{cal}/mol **K_D = 0.112** μM	**ΔG = -10.06** K_{cal}/mol **K_D = 0.042** μM	**ΔG = -10.04** K_{cal}/mol **K_D = 0.044** μM	**ΔG = -8.29** K_{cal}/mol **K_D = 0.837** μM
αPβG	**ΔG = -9.59** K_{cal}/mol **K_D = 0.093** μM	**ΔG = -9.67** K_{cal}/mol **K_D = 0.081** μM	**ΔG = -10.78** K_{cal}/mol **K_D = 0.013** μM	**ΔG = -10.44** K_{cal}/mol **K_D = 0.022** μM
αPβ1-A	**ΔG = -9.75** K_{cal}/mol **KD = 0.071** μM	**ΔG = -9.90** K_{cal}/mol **KD = 0.055** μM	**ΔG = -10.67** K_{cal}/mol **KD = 0.015** μM	**ΔG = -10.70** K_{cal}/mol **KD = 0.014** μM
αPβC	**ΔG = -9.55** K_{cal}/mol **K_D = 0.100** μM	**ΔG = -9.59** K_{cal}/mol **K_D = 0.093** μM	**ΔG = -10.52** K_{cal}/mol **K_D = 0.019** μM	**ΔG = -7.82** K_{cal}/mol **K_D = 1.851** μM

Table 2. *Predicted binding free energies (ΔG) and dissociation constants (K_D) for cRGD and thyroid hormone metabolites docked to human and sea urchin integrin dimers.* ΔG values (kcal/mol) were obtained from PRODIGY for the best model in the top HADDOCK cluster for each integrin–ligand pair. K_D values (μM) were calculated from ΔG using ΔG = RT ln (Kd) with R (gas constant) = 0.001987 kcal·mol^{-1}· K^{-1} and T (absolute temperature) = 298.15 K (25 °C). Ligands include cRGD, rT3, T3, T4, sT3, sT4, TRIAC, and TETRAC.

Across all integrins (Table 2), human αVβ3 displayed the strongest and most consistent binding profile, with cRGD, TRIAC, and TETRAC each showing ΔG ≤ −10.4 kcal/mol and K_D < -0.025 μM. Particularly notable were sT3 and sT4, which bound with ΔG values of −11.46 and −11.07 kcal/mol, respectively, and low-nanomolar K_D values (0.004 μM and 0.008 μM).

Among the sea urchin integrins, αPβ1-A most closely matched the αVβ3 binding profile. It displayed the highest cRGD affinity among all sea urchin candidates (ΔG = −10.13 kcal/mol, K_D = 0.037 μM)

and maintained strong TRIAC, TETRAC, T3, and T4 binding (ΔG between −9.81 and −10.70 kcal/mol and K_D between 0.015 and 0.064 μM). sT3 and sT4 affinities, though slightly weaker than αVβ3, remained in the low-nanomolar range.

αPβG also exhibited consistently strong interactions, with all ligands binding at ΔG ≤ −9.37 kcal/mol and K_D ≤ 0.135 μM, although T3 and T4 affinities were slightly reduced relative to αVβ3. αVβ1-A showed moderate binding strength, binding well with TRIAC and TETRAC but with weaker cRGD (ΔG = −8.89 kcal/mol, K_D = 0.304 μM) and rT3 interactions.

In contrast, βC-containing dimers (αVβC and αPβC) displayed more variable binding. αVβC maintained reasonable affinities for most ligands but showed a significant drop in sT4 binding (ΔG = −8.29 kcal/mol, K_D = 0.837 μM), while αPβC showed strong TRIAC and sT3 binding but much weaker TETRAC (ΔG = −8.36 kcal/mol, K_D = 0.744 μM) and sT4 (ΔG = −7.82 kcal/mol, K_D = 1.851 μM) interactions. αVβG generally exhibited the weakest affinities across all ligands, particularly for cRGD and T3/T4.

Overall, ligand-specific trends reveal that TRIAC and TETRAC consistently bind strongly to most integrins, often achieving ΔG values of −10.0 kcal/mol or better with correspondingly low K_D values. sT3 and sT4 generally emerge as the top binders, particularly in αVβ3 (ΔG = −11.46 and −11.07 kcal/mol; K_D = 0.004 and 0.008 μM) and in top sea urchin candidates such as αPβ1-A and αPβG. cRGD binding is also strong in αVβ3, αPβ1-A, and αPβG, but is noticeably weaker in αVβG and αVβ1-A. rT3 shows more variable performance however, with its affinity in αVβ3 and αPβG comparable to cRGD, whereas βC-containing dimers and αVβG bind rT3 more weakly, with αPβC showing the poorest rT3 binding (ΔG = −7.82 kcal/mol, K_D = 1.851 μM).

Discussion

Structure Modeling Performance of Human and Sea Urchin Integrins

The AlphaFold-Multimer modeling results demonstrate that both the human αVβ3 reference integrin and the six sea urchin integrin heterodimers were predicted with confidence scores that support their use in downstream docking analyses. For human αVβ3, the high ipTM (0.81), pTM (0.82), and pLDDT (81.29) scores, coupled with an RMSD of only 1.052 Å when aligned to the αVβ3 extracellular crystal structure (PDB 1L5G), indicate that the model closely reproduces experimentally determined structural features. This close agreement validates the AlphaFold workflow as an appropriate approach for integrin modeling in this study.

For sea urchin integrins, ipTM and pTM scores ranged from 0.62 to 0.72 and 0.63 to 0.69, respectively, with pLDDT scores between 74.01 and 77.15. Since pLDDT values above 70 indicate confident local structure prediction and ipTM/pTM values above 0.7 are generally considered indicative of reliable overall folds and chain interfaces (Jumper et al., 2021), the majority of the sea urchin models fall within a slightly lower but acceptable quality range. Models with particularly low scores, like αPβC, exhibited higher RMSDs relative to the human αVβ3 template, which may further indicate that they are not valid structural analogs to human αVβ3.

Notably, βC-containing heterodimers (αVβC and αPβC) did not preserve the canonical α–β heterodimer arrangement as well as the other models, with altered domain orientations and partial separation of the headpiece and leg regions. These deviations, along with their slightly lower ipTM/pTM scores, suggest that either modeling uncertainty or genuine structural divergence in βC subunits could be responsible. Additionally, while most sea urchin integrin models retained Mn^{2+} ions at positions equivalent to those in human αVβ3, the αPβ1-A model showed one Mn^{2+} ion positioned differently relative to the canonical metal ion–dependent adhesion site. Such variation

could influence ligand positioning during docking and should be considered when interpreting the binding results.

Despite these differences, the majority of the models preserved the key integrin subunit domains, including the β-propeller and β-I domains in the α-subunits and the β-I, hybrid, and PSI domains in the β-subunits. The overall structural conservation across most models supports their suitability for HADDOCK docking simulations targeting mapped RGD-contacting residues. The variability observed (i.e., in βC-containing dimers) may also provide insight into subunit-specific flexibility and its potential role in modulating ligand-binding behavior in sea urchin integrins.

Docking Performance of cRGD and Thyroid Hormone Metabolites

Binding free energy (ΔG) and dissociation constant (K_D) values from the HADDOCK & PRODIGY workflow reveal distinct differences in the ligand interactions of human αVβ3 and the six sea urchin integrins toward cyclic RGD and the thyroid hormone metabolites. Consistent with its known role as a high-affinity RGD-binding receptor, human αVβ3 demonstrated strong binding to cRGD (ΔG = −9.68 kcal/mol, K_D = 0.080 μM) alongside tight interactions with several thyroid hormone analogs, most notably sT3 and sT4, which displayed low-nanomolar affinities (K_D = 0.004 μM and 0.008 μM, respectively).

Among the sea urchin integrins, αPβ1-A exhibited the closest binding pattern to αVβ3 across the ligand panel. This integrin bound cRGD with higher affinity than αVβ3 (ΔG = −10.13 kcal/mol, K_D = 0.037 μM) and showed ΔG values for TRIAC, TETRAC, T3, and T4 within ~0.1-0.2 kcal/mol of αVβ3. Although sT3 and sT4 binding was slightly weaker than in αVβ3, affinities remained in the low-nanomolar range, supporting αPβ1-A as the most likely structural and functional analog of human αVβ3 in *S. purpuratus*.

αPβG also displayed consistently strong interactions across ligands, with affinities for cRGD and the thyroid hormone analogs remaining sub-micromolar, although T3, T4, and sT4 binding were

modestly weaker than in αVβ3. αVβ1-A showed good cRGD binding and similarity to αVβ3 for TRIAC and TETRAC but had weaker interactions with T3, T4, and rT3.

In contrast, αVβC, αPβC, and αVβG each exhibited one or more major deviations from the αVβ3 binding profile patterns. αVβC maintained reasonable affinities for most ligands but displayed a significant decrease in T4 binding (K_D = 0.837 μM compared to 0.008 μM in αVβ3). αPβC showed strong cRGD and sT3 binding but substantially weaker interactions with TETRAC and sT4. αVβG was generally weaker than αVβ3 across all ligands, particularly cRGD, T3 and T4.

Taken together, the binding affinity data suggest that αPβ1-A is the strongest candidate for a sea urchin integrin structurally analogous to human αVβ3, with αPβG and αVβ1-A as secondary candidates. These findings provide a functional starting point for further structural comparison, particularly focusing on the RGD-binding pocket and metal ion coordination sites.

Context within the Literature

In vertebrates, αVβ3 plays a dual role in RGD-mediated extracellular matrix interactions and non-canonical thyroid hormone signaling and comparable binding patterns in αPβ1-A suggest the evolutionary conservation of at least some aspects of this signaling capacity.

Caveats

This study relies on in silico predictions using AlphaFold models and rigid-body docking with HADDOCK, which may not capture the full conformational dynamics of integrin activation or ligand-induced fit effects. While model confidence scores were acceptable, flexible loop regions and interdomain angles could differ in vivo, influencing binding. Additionally, deviations in heterodimer arrangement in βC-containing integrins and altered Mn^{2+} positioning in αPβ1-A highlight potential uncertainties that may affect docking outcomes. K_D values from PRODIGY are also derived from ΔG under idealized assumptions and have not been experimentally validated.

Future Directions

Experimental validation to test the efficacy of the predicted strongest candidate, αPβ1-A, would be the next step. Expression of αPβ1-A in a recombinant system, followed by binding assays would allow for empirical K_D measurements. Structural determination via cryo-EM or X-ray crystallography could confirm whether the ligand-binding pocket and metal ion coordination resemble αVβ3. Broader ligand screening, including other integrin-targeting peptides and thyroid hormone metabolites, could also help refine the functional similarity assessment. Expression profiling in sea urchin tissues could also establish whether αPβ1-A is positioned to mediate thyroid hormone signaling in vivo, especially given that thyroid hormones have already been shown to bind to sea urchin membrane preparations and influence gene expression ().

Concluding Remarks and Broader Significance

This study identifies αPβ1-A as the most promising sea urchin analog to human αVβ3, supported by both structural modeling and ligand-binding profiles. The integration of AlphaFold modeling with docking analyses demonstrates the utility of computational pipelines for inferring functional analogies in species lacking direct orthologs. More broadly, these results suggest that integrin-mediated, non-canonical thyroid hormone signaling may be an ancient and conserved feature of metazoan biology. Such insights not only advance understanding of integrin evolution but may also inform the design of therapeutics targeting integrin-hormone interactions in human disease.

Integrin	cRGD, rT3, TRIAC, TETRAC	T3, T4, sT3, sT4
Human αVβ3	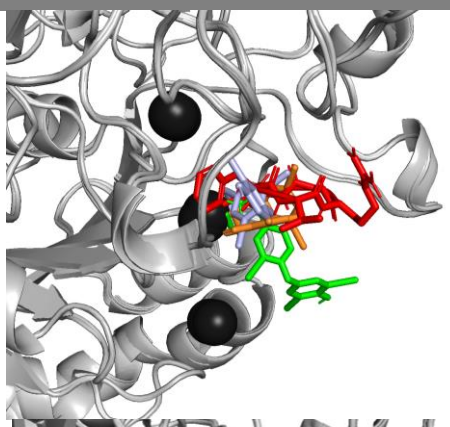 A	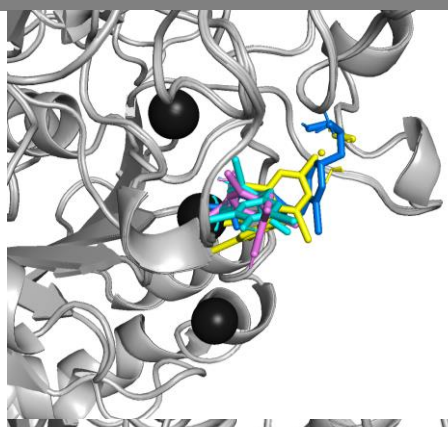 B
Sea Urchin αPβ1-A *(Strongest Candidate)*	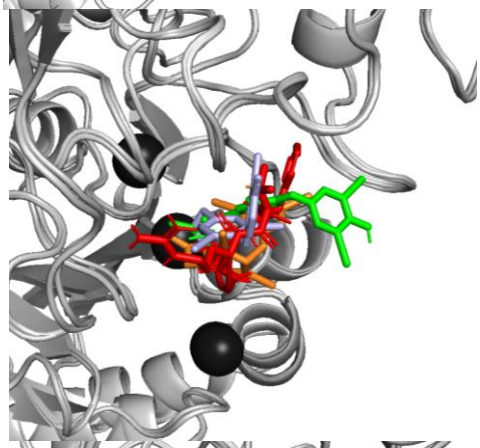 C	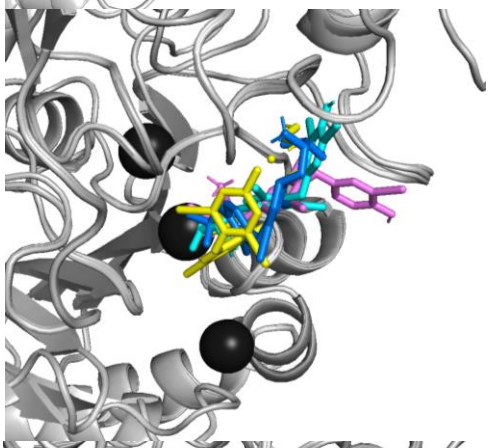 D
Sea Urchin αPβG *(Honourable Mention 1)*	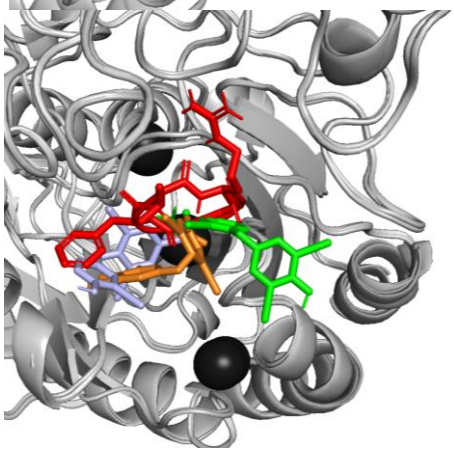 E	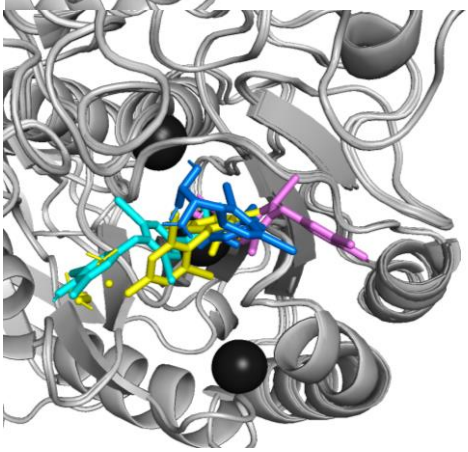 F

Sea Urchin αVβ1-A *(Honourable Mention 2)*

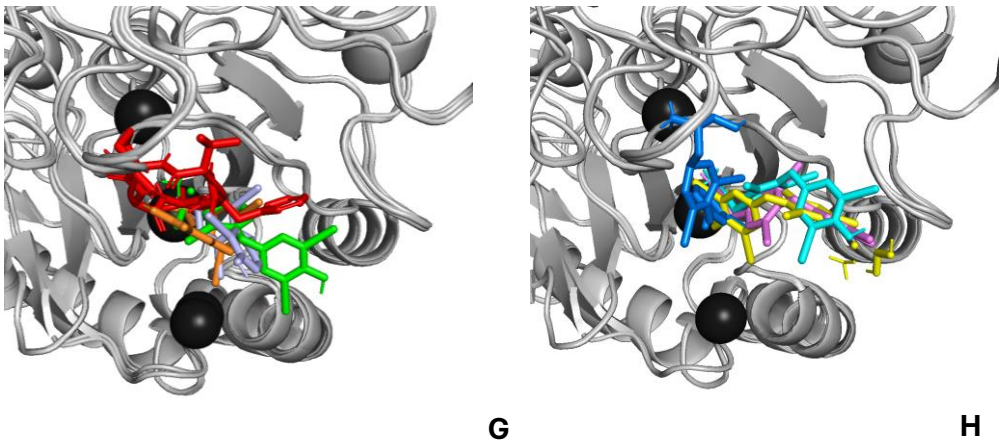

Figure 3. *Comparison of ligand binding poses in human αVβ3 and selected sea urchin integrins predicted to be its closest structural analogs.* Structures show docking results for **(A–B)** human αVβ3, **(C–D)** sea urchin αPβ1-A (strongest candidate), **(E–F)** sea urchin αPβG (honourable mention), and **(G–H)** sea urchin αVβ1-A (honourable mention). Left column (A, C, E, G) depicts cRGD (red) bound alongside rT3 (green), TETRAC (orange), and TRIAC (purple). Right column (B, D, F, H) depicts T3 (pink), T4 (cyan), sT3 (blue), and sT4 (yellow). All ligands dock within the RGD-binding pocket adjacent to the metal ion-dependent adhesion site (black spheres represent Mn^{2+} ions).

References

Borea, P. A., Varani, K., Gessi, S., Gilli, P., & Dalpiaz, A. (1998). Receptor binding thermodynamics as a tool for linking drug efficacy and affinity. *Farmaco (Societa chimica italiana : 1989)*, *53*(4), 249–254. https://doi.org/10.1016/s0014-827x(98)00017-2

Dominguez, C., Boelens, R., & Bonvin, A. M. J. J. (2003). HADDOCK: A protein–protein docking approach based on biochemical or biophysical information. Journal of the American Chemical Society, 125(7), 1731–1737. https://doi.org/10.1021/ja026939x

Jumper, J., Evans, R., Pritzel, A., et al. (2021). Highly accurate protein structure prediction with AlphaFold. Nature, 596(7873), 583–589. https://doi.org/10.1038/s41586-021-03819-2

Ludwig, B. S., Kessler, H., Kossatz, S., & Reuning, U. (2021). RGD-binding integrins revisited: How recently discovered functions and novel synthetic ligands (re-)shape an ever-evolving field. *Cancers, 13*(7), 1711. https://doi.org/10.3390/cancers13071711

Takada, Y., Ye, X., & Simon, S. (2007). The integrins. *Genome Biology, 8,* 215. https://doi.org/10.1186/gb-2007-8-5-215

Taylor, E., Wynen, H., & Heyland, A. (2023). Thyroid hormone membrane receptor binding and transcriptional regulation in the sea urchin *Strongylocentrotus purpuratus*. *Frontiers in Endocrinology, 14,* 1195733. https://doi.org/10.3389/fendo.2023.1195733

Tieman, K. (2025). *Non-canonical thyroid hormone signaling in sea urchin skeletogenesis* (Master's thesis, University of Guelph).

Tobi, D., Krashin, E., Davis, P. J., Cody, V., Ellis, M., & Ashur-Fabian, O. (2022). Three-dimensional modeling of thyroid hormone metabolites binding to the cancer-relevant αvβ3 integrin: In-silico based study. *Frontiers in Endocrinology, 13,* 895240. https://doi.org/10.3389/fendo.2022.895240

Tiwari, S., Askari, J. A., Humphries, M. J., & Bulleid, N. J. (2011). Divalent cations regulate the folding and activation status of integrins during their intracellular trafficking. *Journal of cell science*, *124*(Pt 10), 1672–1680. https://doi.org/10.1242/jcs.084483

Xiong, J.-P., Stehle, T., Zhang, R., Joachimiak, A., Frech, M., Goodman, S. L., & Arnaout, M. A. (2002). Crystal structure of the extracellular segment of integrin αVβ3 in complex with an Arg-Gly-Asp ligand. *Science, 296*(5565), 151–155. https://doi.org/10.1126/science.1069040

Xue, L. C., Rodrigues, J., Kastritis, P. L., Bonvin, A. M. J. J., & Vangone, A. (2016). PRODIGY: A web server for predicting the binding affinity of protein–protein complexes. Bioinformatics, 32(23), 3676–3678. https://doi.org/10.1093/bioinformatics/btw514